A 24-element Silicon PIN diode detector for high resolution radioxenon measurements using simultaneous X-ray and electron spectroscopy

Christopher E. Cox, Wolfgang Hennig, Alan C. Huber, William K. Warburton, Peter M. Grudberg, Stephen J. Asztalos, Hui Tan, Steven Biegalski

Abstract– **The measurement of atmospheric radioxenon is an important tool for monitoring nuclear weapons testing. The development of new and improved xenon detection methods supports the monitoring program of the Comprehensive Test Ban Treaty Organization (CTBTO). In the current work we have developed a 24-element Si PIN diode detector to measure both the characteristic X-rays and the high energy mono-energetic conversion electrons emitted by the xenon radioisotopes. The low noise properties and ultra-thin entrance window of the PIN diodes are well suited for resolving the relatively low energy X-ray lines while simultaneously measuring the high energy conversion electrons with high collection efficiency and near-Gaussian peak shapes. The use of coincidence gating between the X-rays and conversion electrons can further improve the detection sensitivity, which we show to rival the current HPGe and scintillator based xenon detection systems that rely mostly on Gamma-ray and Beta/Gamma coincidence detection, respectively. The Si PIN detector arrangement offers others advantages compared to current xenon detection methods, such as compact construction, intrinsically low background, and the lack of any memory effect from previous measurements. We discuss the construction of the detector and present measurements performed with ^{131m}Xe, ^{133}Xe, ^{133m} Xe and ^{135}Xe. Finally, we make an estimate of the minimum detectable concentration (MDC) for each isotope and compare with the CTBTO requirements.**

I. INTRODUCTION

Detection of atmospheric radioxenon is one of the tools used in nuclear explosion monitoring. The Xe isotope ratios can be used to distinguish nuclear explosions from other sources of radioxenon production such as nuclear power plants or radiopharmaceutical facilities. Besides generally improving the sensitivity (i.e., lowering the background or increasing the efficiency of the detector), distinction of isotopes can be achieved by improving the detector's energy resolution so that key X-ray lines from the different isotopes no longer overlap in the energy spectra. High energy resolution therefore emerges as a desirable feature in future detectors deployed at the Comprehensive Test Ban Treaty Organization International Monitoring Stations.

In the case of weak radioisotope activity, it is advantageous to resolve closely spaced X-ray lines and collect gamma emissions in the same detector. Although gamma-ray absorption in a silicon detector is unacceptably low, the xenon isotopes emit conversion electrons equal to the gamma energy less the electron binding energy, (Table I). Conversion electron spectroscopy therefore offers an alternative to gamma-ray detection, especially when the radioisotope under investigation is in the form of a gas, in which case self-absorption of conversion electrons in the source material is minimized. For radioxenon monitoring, silicon X-ray detectors offer the features of low noise and highly resolved X-ray peaks in the range 2 keV – 40 keV and high collection efficiency (stopping power) for conversion electrons up to few hundred keV.

Earlier studies [1]-[5] examined the results of irradiating silicon detectors with mono-energetic conversion electrons. In later work [6], [7] we tested state-of-the art high resolution silicon X-ray detectors and performed electron spectroscopy in the range 45 keV – 300 keV with relatively low cost commercially available Si PIN diodes. The ultra-thin entrance window of these detectors, (originally developed for low energy X-ray spectroscopy), and the short stopping distance of electrons in silicon resulted in a high collection efficiency and near-Gaussian spectrum peaks for the high energy conversion electrons. Recent work by Peräjärvi et al [8] achieved similar results with Silicon Drift Detectors.

The use of silicon detectors offers several advantages over existing radioxenon detection systems based on scintillators (beta-gamma detection) or HPGe gamma detectors. These advantages include:

- a relatively compact design,
- improved energy resolution for K X-rays,
- ability to use additional L X-rays,
- low background (no shielding required),
- no memory effect from absorbed xenon.
- Coincidence gating between X-rays and electrons.

Manuscript received November 8, 2013. This work was supported by the U.S. Department of Energy under Award No. DE-SC0004272.

C. E. Cox is with XIA LLC, Princeton, NJ USA (tel 609-279-1552, e-mail: ccox@xia.com)

W. Hennig is with XIA LLC, Hayward, CA USA (tel 510-401-5760, e-mail whennig@xia.com)

W. K. Warburton is with XIA LLC, Hayward, CA USA (tel 510-401-5760, e-mail bill@xia.com)

A. C. Huber is with Amptek Inc, Bedford, MA USA (tel 781-275-3470, e-mail ahuber@amptek.com)

P. M. Grudberg is with XIA LLC, Hayward, CA USA (tel 510-401-5760, e-mail peter@xia.com)

S. J. Asztalos is with XIA LLC, Hayward, CA USA (tel 510-401-5760, e-mail steve@xia.com)

H. Tan is with XIA LLC, Hayward, CA USA (tel 510-401-5760, e-mail htan@xia.com)

S. Biegalski is with the University of Texas at Austin, TX USA (tel 512-232-5380, e-mail biegalski@mail.utexas.edu)

978-1-4799-0534-8/13/$31.00 ©2013 IEEE

Isotope	Energy (keV)											
	L X-rays		K X-rays				Conversion Electrons					Gammas
^{135}Xe	4.3	4.7	30.6	31.0	35.0	36.0	214	244				250
^{133m} Xe	4.1	4.5	29.4	29.8	33.6	34.6	199	228	232	233		233
^{133}Xe	4.3	4.7	30.6	31.0	35.0	36.0	45	75	76	80		81
^{131m}Xe	4.1	4.5	29.4	29.8	33.6	34.6	129	158	159	163	164	164
^{127}Xe	3.9	4.3	28.3	28.6	32.3	33.0	24	112	139	170	198	172, 203, 375

Table I: X-ray, Conversion Electron and Gamma-ray energies from Radioxenon.

However, there are significant challenges to be overcome in the construction and testing of a practical, field-deployable system, such as

- encapsulation of the gas,
- placement of the PIN diodes to optimize efficiency,
- reducing electronic noise and low energy threshold,
- cooling the detector array to reduce leakage current,
- mitigating signal cross-talk between channels.

In the current work we describe the construction of a 24-element PIN diode detector and our solutions to the various engineering difficulties mentioned above. We present conversion electron and X-ray spectra from measurements with ^{127}Xe, ^{131m}Xe, ^{133}Xe, ^{133m} Xe and ^{135}Xe, and demonstrate detection of ^{37}Ar from the low energy X-ray peak at 2.6 keV. Both one-dimensional and coincidence-gated spectra are presented. The minimum detection limit of ^{133}Xe from the 24-element detector is estimated to be 0.1 mBqm^{-3} for a 24-hour sampling time. This compares with the CTBTO requirement of < 1 mBqm^{-3}.

II. TWO-ELEMENT PROTOTYPE DETECTOR

Before proceeding with the 24-element detector, a prototype device was constructed from just two 25 mm^2 PIN diodes. The main purpose was to check the fabrication and performance of a custom PIN diode ceramic mount, (provided by Amptek Inc). The completed prototype also served as a test bed for many of the construction techniques and the coincidence gating method used in the final detector.

Fig. 1a is a photograph of one 25 mm^2 PIN diode mounted on the custom alumina support. Vias in the alumina take the HV and anode bonded wires through to the rear side of the support, where the FET and external signal connections are mounted. The PIN diode chip and FET are standard production devices; only the mounting was customized.

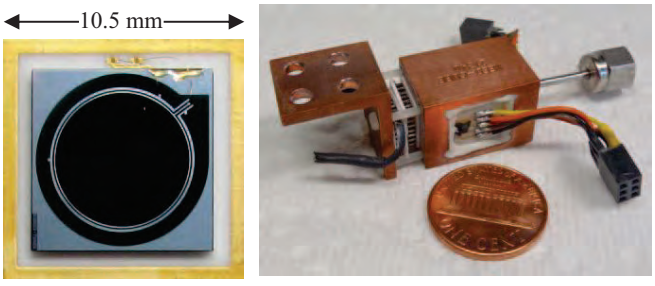

a. b.

Fig 1. a) 25-sqmm PIN diode mounted on custom ceramic support. b) Gas encapsulation cuboid for the prototype detector, showing the back of the PIN diode, the Peltier cooler, and the gas inlet tube.

Fig. 1b shows the Xe encapsulation volume for the prototype detector, consisting of a copper cuboid with internal volume 1000 mm^3 (1 cm^3) and two 25 mm^2 diodes glued into appropriately sized openings in the sides of the copper. The spacing between the diode chips inside the cuboid was 10 mm. The external connecting wires for the preamplifiers are visible, as are the FET (protected by black sealant) and the external Peltier cooler and heat sink. Xe gas was introduced through a 1.6 mm OD stainless steel tube that was first glued, and later brazed, onto the copper. An important design feature of the cuboid is that the internal volume is vacuum tight, thereby fully encapsulating the gas under test.

The ceramic mount for the diodes formed an interference fit in the copper cuboid. After some trials, Armstrong A12 epoxy was selected to hold the diodes in place and create the vacuum seal around the edges.

The copper cuboid assembly was mounted with the signal preamplifiers inside an airtight and light-tight Aluminum housing that was flushed with dry N_2 gas to stop water vapor condensation on the PIN diode outer surfaces when cooled. The operating temperature of the copper cuboid was approximately 280K, which provided sufficient cooling of the PIN diodes to achieve an energy resolution of 700-800 eV FWHM at the 30keV Xe doublet peaks. A further discussion of the dependency of the energy resolution on operating temperature and other factors is presented in section IV.

Fig. 2 is the energy spectrum from ^{131m}Xe collected with the prototype detector during tests at the Pacific Northwest National Lab, displayed with and without coincidence gating between X-rays and conversion electrons. For these measurements, the cuboid was first evacuated and then backfilled with Xe gas to less than one atmosphere pressure. The data was collected in list mode using the xMAP spectrometer from XIA, and the gating performed in post-measurement analysis. The conversion electron peaks at 129, 159 and 163 keV are clearly visible in Fig. 2, as are the lower energy X-ray peaks. Elsewhere [9] the minimum detectable limit (MDC) of the prototype detector for most of the xenon radioisotopes was calculated to be in the range 4–25 mBq/m^3 for a 24 hour sampling time, compared to the CTBTO monitoring station requirement of <1 mBq/m^3.

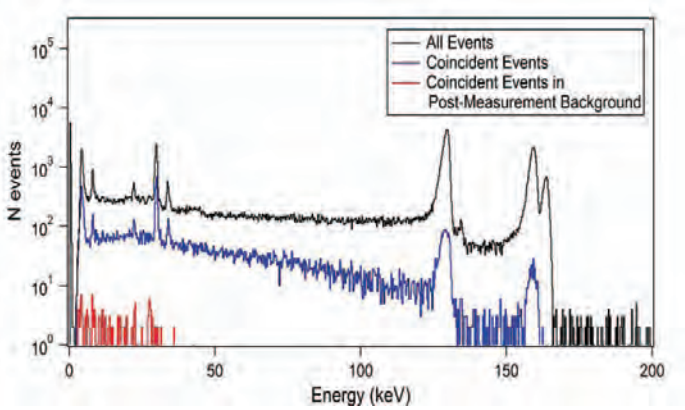

Fig 2. ^{131m} Xe spectrum from prototype 2-sided 25-sqmm Si PIN diode detector, with and without coincidence gating.

Having proved the efficacy of the custom PIN diode mount, the gas encapsulation method, the detector cooling, and the coincidence gating, a major goal of the work was to increase the xenon detection sensitivity to meet or exceed the CTBTO requirements.

III. Mechanical Layout of the 24-Element Detector

A. Gas encapsulation.

The final detector design employed 4x25 mm^2 PIN diodes on each of 6 sides of a cuboid made from OFHC copper, giving a total active area of 600 mm^2 compared to 50 mm^2 in the prototype. In an ideal detector the inactive area is minimized by making the space between the 25 mm^2 elements as small as possible. To this end, our initial concept was to modify the ceramic mount to hold 4 PIN diode chips on a common support, as shown in Fig. 3a. A number of these quad-type detectors were manufactured, but problems with the chip bonds and a poor detector leakage current yield led to the abandonment of this approach. Instead, we fabricated "window frames" holding 4 PIN diodes (Fig. 3b), which were mounted on the same type of individual ceramic mounts used in the prototype detector.

Fig. 4 shows the partially constructed 24-element cuboid. Spacing between the PIN diodes is not ideal, but is a compromise to accommodate the proven technology of the individual ceramic mounts. For this design, the total internal volume is 16500 mm^3 (16.5 cm^3).

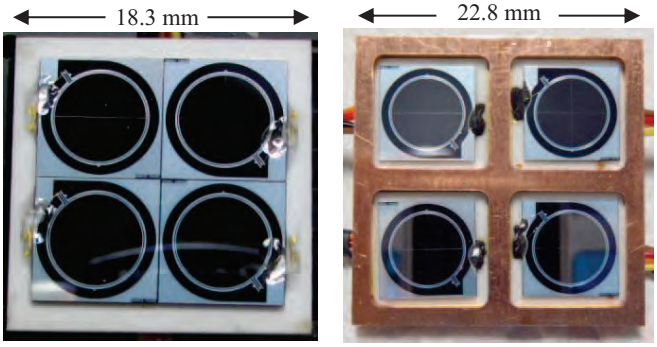

a. b.

Fig 3. a) Attempt at a quad PIN diode structure mounted on a common ceramic support. This technique was abandoned due to poor yield. b) "Window frame" of 25 mm^2 PIN diodes mounted on individual ceramic supports, as used in the final detector design.

Fig 4. Inside view of the partially constructed detector cuboid, showing three window frames glued in place and the gas inlet hole, (visible near the center of the picture).

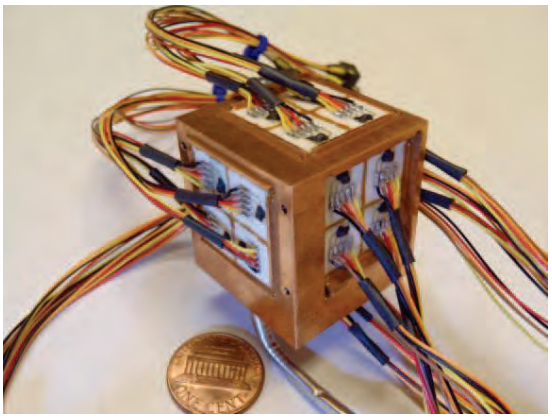

Fig 5. Outside view of the completed detector cube.

Fig. 5 is an outside view of the completed detector cuboid showing the external wiring for the 24 preamplifiers. A 3.2 mm OD stainless steel tube was brazed into the copper to provide the gas inlet. As with the prototype, an important requirement is the vacuum tightness of the completed cuboid to eliminate unwanted gas (e.g., N_2 or air) leaking in during a measurement. A leak rate of less than 10^{-2} mbar/l-s was acceptable, which was easily detectable by a commercially available He leak checker. As in the prototype detector, for the limited temperature range of this design it was found that Armstrong A-12 epoxy formed an adequate seal for gluing the individual PIN diodes and the window frames. The weakest link in the vacuum plumbing was in fact the Swagelok pipe connectors, which needed considerable tightening to provide a reliable vacuum seal.

B. External housing.

The copper cuboid was mounted in an airtight and light-tight aluminum container (Fig. 6) that also housed the Peltier coolers to attain a detector operating temperature of about 280K. Prior to operation, the container was flushed with dry N_2 gas to eliminate condensation on the cooled surfaces.

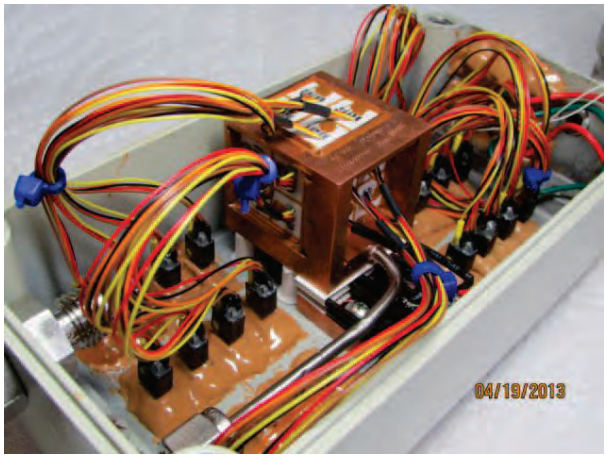

Fig 6. Detector cube mounted inside sealed box, (lid removed)

The aluminum box also provided electrical screening for the sensitive FET and feedback components that are mounted on the outside surface of each PIN diode. The preamplifiers were mounted on the outside of the box and wired to the detectors through sealed 6-pin connectors. Fig. 7 shows the completed detector assembly with ribbon connectors from the preamps to a signal and power distribution board, which routed the 24 output signals to SMA connectors.

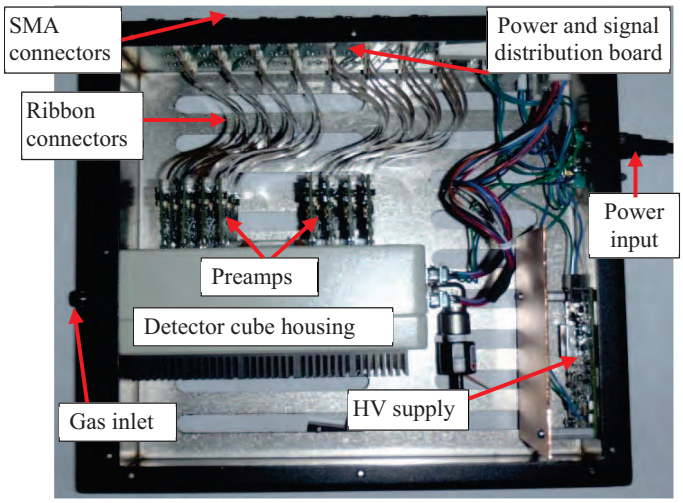

Fig 7. Complete detector assembly, (with lid removed).

IV. Noise and Energy Resolution Considerations

The noise and energy resolution of the PIN diode array can be affected by several factors, including:

- Operating temperature of the diodes and FETs.
- Detector leakage currents.
- 1/f noise from FET and bond wire encapsulation.
- Unresolved $K\alpha_1$ / $K\alpha_2$ doublet peaks.
- Cross-talk between channels

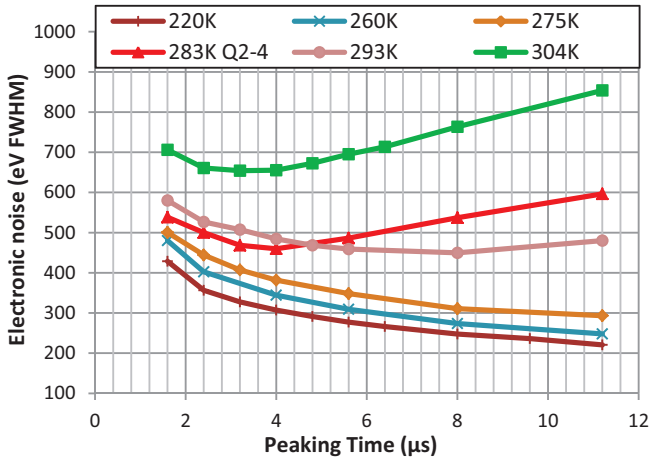

Fig. 8. Electronic noise vs. pulse processor peaking time for a 25-sqmm PIN diode at various temperatures.

Fig. 8 is a plot of electronic noise versus processor peaking time for a 25-sqmm PIN diode at various operating temperatures. The increase in noise at long peaking times was due to detector leakage current. Five of the curves in the plot were derived from an off-the-shelf 25-sqmm PIN diode, of a similar type to that used in the array but mounted in a standard TO8 package with a beryllium window. The red line is from a PIN diode in the 24-element array. In our arrangement we chose to operate between 280-285K to simplify the cooling requirements and to reduce the risk of water vapor condensation on the detector cube. The optimum peaking time was 4µs. Note that the leakage current noise was somewhat higher for the array detector than the equivalent measurement for the standard sealed detector, which may be a result of operating the diode outside of its factory-sealed environment.

There was also a 1/f component of noise for all the measurements, which for a given temperature can be derived from Fig. 8 after removing the leakage current noise. The array diode (red line) was found to have a 1/f noise value of 320 eV FWHM, which compares to 195 eV FWHM for the standard diode at a similar temperature. The increase in 1/f noise is most likely due to a protective encapsulation material that was pasted over the sensitive FET, bond wires and feedback components.

One goal of the detector design was to resolve the K X-rays emitted by the ground and metastable states of the Xe isotopes around 30 keV. Referring to Table I, the K X-ray lines in question are separated by 1200 eV, and therefore should be easily resolvable by the PIN diodes. However, the $K\alpha_1$ and $K\alpha_2$ lines form an unresolved doublet that broadens the ground state and metastable state Kα peaks, making them harder to resolve. To illustrate this point, Fig. 9 is a plot of the 283K noise data from Fig. 8 (red line) displayed with the theoretical resolution of a singlet peak at 30 keV and the expected (modeled) resolution of the $K\alpha_1/K\alpha_2$ doublet. It can be seen that the doublet increases the calculated resolution of the Kα peaks to 700 eV FWHM, making the metastable and ground state isotopes only just resolvable with the PIN diode detector.

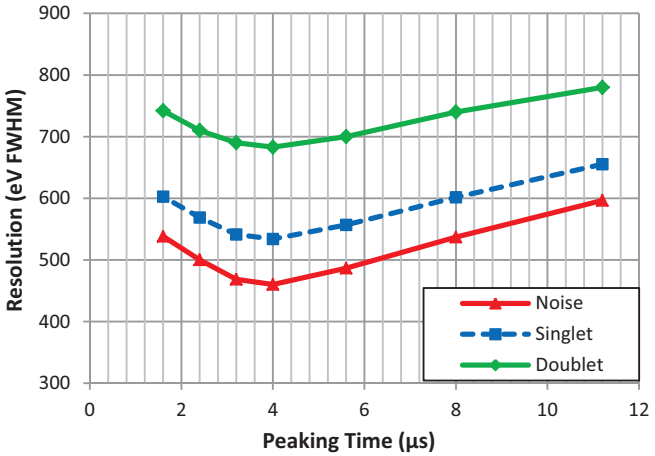

Figure 9. 25-sqmm PIN diode noise and resolution at 283K vs. peaking time. Red: Measured electronic noise.
Blue: Calculated resolution for a single peak at 30 keV.
Green: Calculated resolution for the $K\alpha_1/K\alpha_2$ doublet at 30 keV.

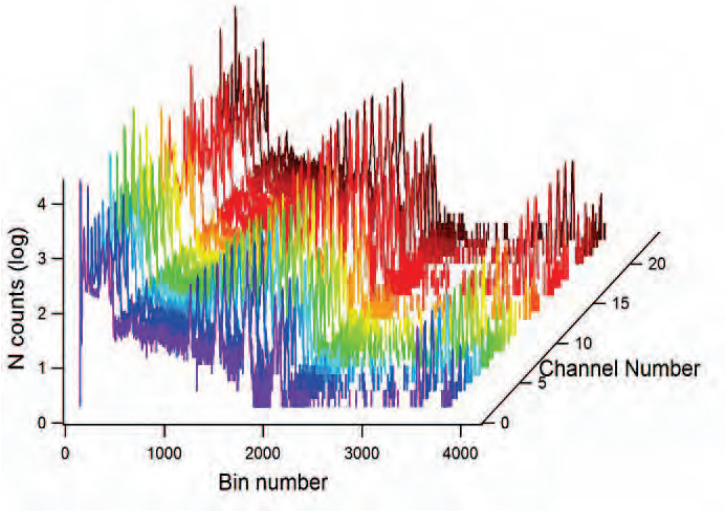

Fig. 10. Superposition of spectra from all PIN diodes for $^{127}Xe + ^{37}Ar$

One of the challenges of any multi-element detector array is the effect of cross-talk between the detector channels. This is commonly experienced with a Reset type FET and preamplifier where a relatively large current is periodically injected into the feedback capacitor to maintain the preamplifier output within the desired voltage limits. The transient current in the FET drain during the reset period can induce, through capacitive coupling, a small voltage step on the preamplifier signal of an adjacent PIN diode. Crosstalk therefore produces parasitic low energy peaks in the spectra that can mask genuine low energy events and raise the effective low energy operating threshold. To prevent this problem, a gating logic signal was generated for each detector channel during the reset period. The gating signals of all channels were summed together (logical "OR") to inhibit data collection during a reset from any PIN diode. Although affective in reducing cross-talk, this technique has the disadvantage of increasing the total dead-time due to the frequent reset periods. At low count rates, the dead-time increase is dependant mostly on the PIN diode leakage currents. For example, if the average time between resets for each of the 24 PIN diodes is 5 ms, (corresponding to a leakage current of 80 pA), and the reset duration is 10µs, then the reset inhibit increases the dead-time by an additional 5%.

V. MEASUREMENTS WITH RADIOXENON

Radioxenon samples were prepared at the University of Texas Nuclear Engineering Test Laboratory in Austin, TX, USA. The isotopes generated at the research reactor were ^{131m}Xe , ^{133}Xe, ^{133m}Xe, ^{135}Xe, and ^{127}Xe mixed with ^{37}Ar. Although ^{127}Xe is not of interest for nuclear non-proliferation, it provided many conversion electron peaks over a wide range of energies and was a useful tool for detector evaluation. ^{37}Ar is generated by neutron activation of Ca in the surrounding rock in an underground nuclear explosion, and is therefore also an isotope of interest to the CTBTO. It is detected by the K X-ray line at 2.6 keV, which was a further test of the detector's low energy sensitivity.

Prior to introducing the gas sample, the detector volume was pumped and back-flushed with dry nitrogen several times to remove water vapor. The Xe samples under test were prepared in a sealed volume of approximately 560 mm^3 (0.56 cm^3), which was expanded through thin stainless steel tubing into the detector cuboid volume. The resulting pressure in the detector was approximately 22 mbar, (2% of atmosphere).

Fig. 10 is a superposition of spectra from all PIN diodes from the $^{127}Xe + ^{37}Ar$ sample. For our analysis it was convenient to sum the digital outputs of all the detector channels after pulse processing, (and after making fine adjustments to the gain.) It should be noted, however, that there were three PIN diodes that developed unacceptably high leakage currents with reset rates less than 1 ms. A few other channels had low energy (<1keV) parasitic peaks that were not removed by reset gating, and whose origin has not yet been determined. These "noisy" channels were not included in the summed spectra shown in Figs. 11-16.

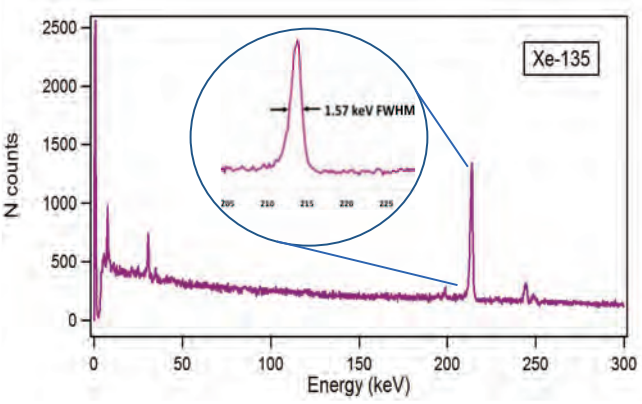

Fig. 11. Sum of spectra from ^{135}Xe sample.

Fig. 11 is the sum of spectra collected from ^{135}Xe and shows the conversion electron peak at 214 keV with resolution 1.57 keV FWHM, compared to a theoretical value of 860 eV FWHM. There is still some broadening due to the combined effect of multiplets in the electron peak, electron absorption in the gas sample and the entrance window of the detector, and possibly electron backscatter from the detector. Nevertheless, this is an excellent result, and demonstrates the clear measurement of conversion electron peaks for our detector arrangement. The electron peaks from ^{131m}Xe are shown in Fig. 12, as well as the K and L X-rays.

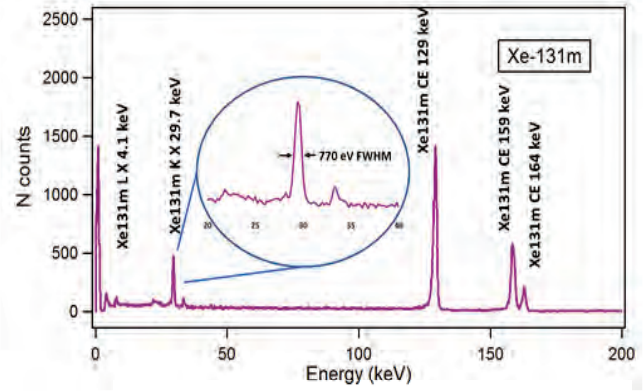

Fig. 12. Sum of spectra from ^{131m}Xe sample.

Note that the sum of the Kα lines from the individual detectors gave a resolution of 770 eV FWHM, which was about 10% higher than our earlier prediction in Fig. 9. This may be due to the addition of some less-than-perfect detector channels, and some slight broadening from the gain adjustment and digital summation process.

The spectrum in Fig. 13 was collected with a mixture of ^{133}Xe and ^{133m} Xe, and shows the overlapping K X-ray lines around 30 keV, separated by 1200 eV. As mentioned in section IV above, the ground and metastable states are only just resolvable, but nevertheless two peaks are clearly visible, and deconvolution software would aid the identification process further. The visible tailing on the conversion electron peak at 45 keV demonstrates that electron absorption in the gas and the PIN diode entrance window dead-layer becomes more pronounced at lower energies. The best-case theoretical resolution at 45 keV is 570 eV FWHM, compared to the measured electron peak width of 1.34 keV.

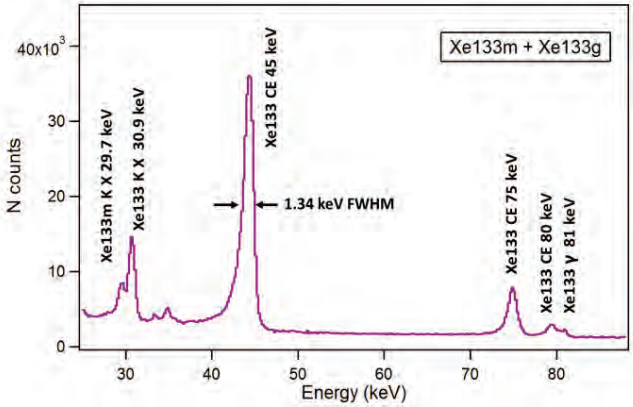

Fig. 13. Sum of spectra from ^{133}Xe and ^{133m}Xe mixture.

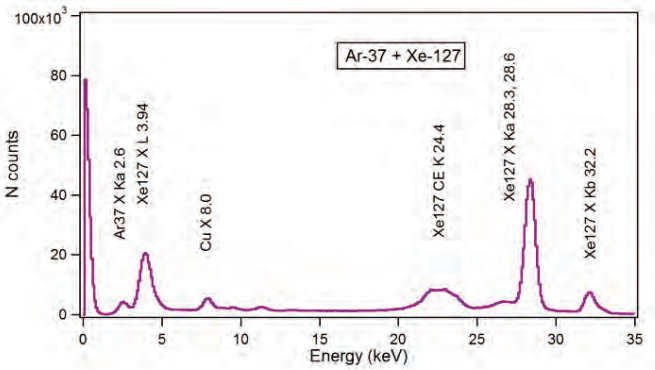

Fig. 14. Sum of spectra from ^{127}Xe and ^{37}Ar mixture.

Fig. 14 is the low energy portion of the ^{127}Xe and ^{37}Ar mixture. Note that the electron peak at 24 keV, (which is a combination of Auger and conversion electrons), is degraded and shifted in energy to due to absorption in the gas and the detector dead-layer. This represents the low-energy threshold for electron spectroscopy. For the low energy X-rays, the ^{127}Xe L multiplets at 4 keV are easily detected, as is the ^{37}Ar K X-ray at 2.6 keV.

VI. COINCIDENCE GATING

Another feature of our multi-element cube is the ability to perform coincidence gating between the PIN diodes. Fig. 15 is a 2-D coincidence plot from the ^{127}Xe and ^{37}Ar data. Each dot represents an event in any PIN diode occurring in coincidence with a second event in any other PIN diode. The dot is placed at the intersection of the two energies involved. We can see, for example, the strong coincidence between X-ray lines at 30 keV and the CE electrons at 112, 139, 170 and 198 keV, and also between the 139 and 170 keV events.

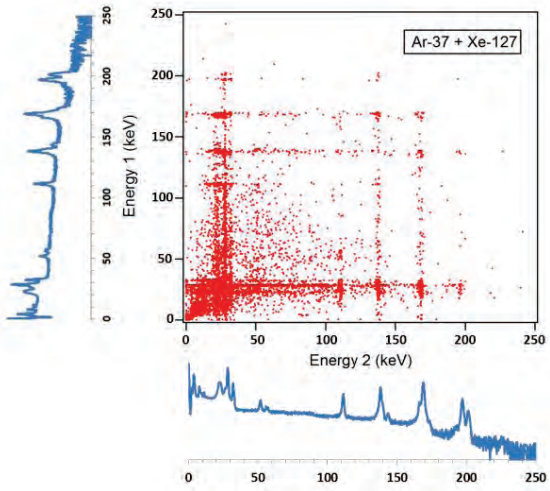

Fig. 15. 2D coincidence plot from ^{127}Xe + ^{37}Ar mixture

In principle, coincidence gating can be used to reduce events from natural background, and is most effective when the solid angle of the active detector area is close to 4π. In the case of the PIN diode array, the natural background is already very low, (about 0.02 cps per detector), so the benefit of reducing the background further is limited. Also, in the present diode

configuration the solid angle for an event at the center of the cube volume is about 2 steradians, which is far short of the ideal 4π. The result is that the overall count rate for coincidence gated events is greatly reduced. Fig. 16 is a comparison of gated and un-gated spectra for the ^{133}Xe and ^{133m}Xe mixture; the reduction in count rate in very marked.

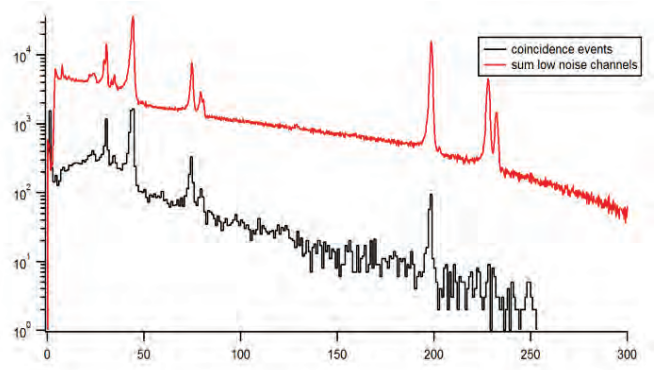

Fig 16. Spectrum from the ^{133}Xe and ^{133m}Xe mixture, with and without coincidence gating.

VII. ESTIMATE OF MEASUREMENT SENSITIVITY

The International Monitoring System Minimum Detectable Concentration (MDC) requirement is defined for ^{133}Xe as less than 1 mBqm^{-3} in a 24 hour sampling period. An absolute efficiency analysis was used to calculate the MDCs from the data collected at the University of Texas. In Table II the MDCs are compared to those from an existing SAUNA system [10], which uses NaI(Tl) and plastic scintillators for Beta/Gamma coincidence gating. It can be seen that the diode array offers roughly a factor of two improvement in MDC for ^{133}Xe (the most abundant isotope), but is worse for the other Xe isotopes.

A denser arrangement of PIN diodes would improve the active area fraction and thus lower the MDC. Note that these MDCs are given for pure isotopes. In practice, samples often contain ^{133}Xe and one or more of the metastables. In the SAUNA system, the spectrum peaks from the metastables are not resolvable from those for ^{133}Xe, so ^{133}Xe adds significant background to the measurement of metastables, and therefore their MDCs are higher in the presence of ^{133}Xe. In the Si system, the metastables' peaks are much sharper and therefore their MDCs are much less affected by the presence of ^{133}Xe.

	MDC for 24 hr sample period. (mBqm^{-3})	
Isotope	24-PIN diode array	SAUNA system
^{131m}Xe	0.72	<0.2
^{133m} Xe	0.65	<0.2
^{133}Xe	0.11	0.18
^{135}Xe	1.3	<0.7

Table II. Comparison of MDCs for the PIN diode array and the SAUNA system.

CONCLUSIONS

A 24-element PIN diode detector has been constructed and tested for the measurement of radioxenon using conversion electrons and X-ray emissions. The detector demonstrated high absorption efficiency and high energy resolution for both X-rays and conversion electrons, and the metastable isotopes could be clearly distinguished even in the presence of ^{133}Xe. The detection of ^{37}Ar was also demonstrated.

Further work to improve the detector performance could include:

- Packing the PIN diodes closer together to improve the solid angle (and MDC).
- Applying a thin (few μm) Parylene coating on the PIN diodes to protect against potential contamination and leakage current degradation.
- Identification (and elimination) of the sources of excess 1/f noise.
- Replacing the 4x25 sqmm PIN diode quad structures with 100 sqmm SDDs to the improve solid angle. (This approach is currently prohibited by the cost of the SDDs).

ACKNOWLEDGEMENTS

The authors are indebted to Derek Haas at PNNL for his assistance in the measurement and analysis of data collected at both PNNL and the University of Texas, and to William Wilson at the University of Texas for his absolute efficiency calculations.

REFERENCES

[1] I. Ahmad and F. Wagner, "A simple cooled Si(Li) electron spectrometer," *Nucl. Instrum. Meth.* vol. 116, p465, 1974.

[2] Y. Shiokawa and S. Suzuki, "Application of internal conversion electron spectrometry to analysis of a ^{243}Cm/^{244}Cm mixture," *J. Radioanal. Nucl. Chem, Articles,* vol. 102, no. 1, pp 239-246, 1986.

[3] I. Ahmad, R.R. Betts, T. Happ, D.J. Henderson, F.L.H. Wolfs, A.H. Wuosmaa, "Nuclear spectroscopy with Si PIN detectors at room temperature", *Nucl. Instr. Meth. A*, vol. 299, pp 201-204, Dec. 1990.

[4] P. Bauer and G. Bortels, "Response of Si detectors to electrons, deuterons and alpha particles," *Nucl. Instr. Meth. A*, vol. 299, pp 205-209, Dec. 1990.

[5] S. Antman and B. Svahn, "Silicon detector response functions to mono-energetic positrons", *Nucl. Instr. Meth.* vol. 82, pp 24-28, May 1970.

[6] C.E. Cox, S.J. Asztalos, W. Hennig, W.K. Warburton, "Electron response in windowless Si(Li), SDD and PIN diode photodetectors", *IEEE Nucl. Sci. Symp. 2011, conference record.*

[7] W. Hennig, C. E. Cox, S. J. Asztalos, H. Tan, P. J. Franz, P. M. Grudberg, W. K. Warburton, A. Huber, "Study of silicon detectors for high resolution radioxenon measurements". *J Radioanal Nucl Chem* Vol 296 No2, May 2013.

[8] K. Peräjärvi, J. Turunen, S. Ihantola, V. Kämäräinen, R. Pöllänen, T. Siiskonen, H. Sipilä, H. Toivonen, "Feasibility of conversion electron spectrometry using a Peltier cooled silicon drift detector", *J Radioanal Nucl Chem*, Oct 2013, submitted for publication.

[9] W. Henning, C.E. Cox, S.J. Asztalos, H. Tan, P.J. Franz, A. Xiang, P. M. Grudberg, W.K. Warburton, A. Huber, S. Biegalski, A. Brand, D, Hass, "Radioxenon measurements with a coincidence detector system", presented at the 2012 International Noble Gas Experiment Workshop, Mito City, Japan.

[10] A. Ringbom, A., T. Larson, A. Axelson, K. Elmgren, and C. Johansson (2003). SAUNA—a system for automatic sampling, processing and analysis of radioactive xenon, *Nucl. Instr. and Meth. A* 508: 542–553.